J. Phys. B: At. Mol. Phys. **14** (1981) 3733–3760. Printed in Great Britain

Electron impact ionisation of Li-like and Be-like ions

H Jakubowicz and D L Moores

Department of Physics and Astronomy, University College London, Gower Street, London, WC1E 6BT, England

Received 3 December 1980, in final form 15 April 1981

Abstract. Electron impact ionisation cross sections for positive ions in the Li and Be isoelectronic sequences are calculated in the Coulomb–Born exchange and distorted-wave exchange approximations using close-coupling wavefunctions to represent the initial and final states of the target system. The corresponding ionisation rate coefficients are also computed as a function of temperature. The results obtained are compared with experiments, with the infinite-Z method of Golden and Sampson and with the Lotz semi-empirical formula. For C, N, O and Ne ions the mutual agreement is better than 25% and in some cases is of the order of a few per cent. For Fe^{23+} and Fe^{22+} the Lotz formula gives rates up to 40% higher than the Coulomb–Born at high temperatures ($>10^8$ K), indicating that the formula probably gives an inaccurate estimate of the high-energy behaviour of the cross section for these ions.

1. Introduction

In the study of astrophysical plasmas such as the solar corona and laboratory plasmas such as those used in fusion research, knowledge of ionisation balance curves giving the relative abundance of the different ionisation stages of each element as a function of temperature, and perhaps time, is required. The ionisation balance calculations in turn require reliable values for the electron impact ionisation cross sections of positive ions and the use of ionisation balance curves based on different approximate cross sections may lead to conflicting conclusions about the physical properties of the plasma being studied (Cheng *et al* 1979). For example, the calculations of Summers (1974), which use ionisation cross sections calculated by the exchange classical impact parameter method (ECIP), predict the ionisation equilibrium temperature of Fe XXI to be 2×10^7 K, a factor of two higher than that predicted by Jordan (1970) using the semi-empirical formula of Seaton (1964) or by Jacobs *et al* (1977) using the Lotz (1967) formula. This lower value is more consistent with the result obtained by Cheng *et al* (1979) from the width of the forbidden line Fe XXI 1354 Å observed in solar flare spectra from Skylab. The various ionisation balance calculations also employ different recombination rates, so that the discrepancies are not necessarily simply a result of the differences in the ionisation rate coefficients. However, Burgess *et al* (1977), by comparing the available experimental and theoretical data concluded that the ECIP method gives results which are in marginally better agreement with experiment than those of other theoretical methods, including *ab initio* quantum mechanical approximations; however, this study was restricted to ions of low charge only. In order to shed some light on these discrepancies, we will address ourselves in this paper to the problem

0022-3700/81/193733+28$01.50 © 1981 The Institute of Physics

of obtaining reliable ionisation cross sections by quantum mechanical techniques and giving estimates of their accuracy.

The various problems which arise in the quantum theory of ionisation and which distinguish it from other processes have been considered by Peterkop (1961, 1977 and references therein), Rudge and Seaton (1965) and Rudge (1968). The source of the difficulties is the long-range nature of the Coulomb potential which ensures that the continuum electrons continue to interact with the residual ion and with each other, even out to infinity, thereby necessitating a full solution of the three-body problem in the asymptotic region. As yet there is no satisfactory method of overcoming this problem and it is necessary to approximate the asymptotic region by neglecting correlations between the continuum electrons. The most commonly used quantum mechanical approximation is the Coulomb–Born approximation (see for example Rudge 1968) in which the ionising electron is described by a Coulomb wavefunction and the ionisation process is depicted as a bound–free transition of the target ion provoked by electron impact. The incorrect description of the asymptotic region in this method results in an asymmetric treatment of the continuum electrons and causes problems in the inclusion of exchange, which must then also be approximated. The validity of the Coulomb–Born approximation, and its various exchange derivatives for positive ions has been discussed by Jakubowicz and Moores (1980). The results of the Coulomb–Born exchange approximation for ionisation of He^+ (Rudge and Schwartz 1966) are in excellent agreement with experiment (Dolder *et al* 1961, Peart *et al* 1969) and it is expected that the accuracy of this approximation will improve with increasing charge of the ion.

In the case of ionisation of complex ions the ionisation process can proceed by inner-shell ionisation, ionisation via autoionising states and simultaneous ionisation and excitation in addition to the simple knockout process in which a valence electron is dislodged from the ion by the impact of the ionising electron. These additional processes can give rise to significant changes in the ionisation cross section (Moores and Nussbaumer 1970). Until now, with the exception of the high-energy Coulomb–Bethe approximation (Kim and Inokuti 1971, Kim and Cheng 1979), which relies on closure for its validity, and in principle the optical potential approach, these processes have only been accounted for in theoretical calculations by the addition of the appropriate cross sections, obtained from independent calculations, to the naked cross section describing only the knockout process. For example, autoionisation is accounted for by adding the relevant excitation cross sections to the undressed ionisation cross sections under the assumption that all the excited states decay into the continuum (see for example Henry 1979, Sampson and Golden 1979, Moores 1979). The possibility that the excited state of the ion may radiatively decay to a bound state before autoionising has been taken into account by multiplying the excitation cross section by the branching ratio $A_a/(A_a+A_r)$, A_a and A_r being the transition probabilities for autoionisation and radiative decay respectively (Cowan and Mann 1979). These types of calculation neglect the quantum mechanical interference which may arise between the various contributing processes and, in the case of autoionisation, since the excitation cross sections are calculated assuming the excited states to be purely bound, do not account for the finite width of the autoionising state. The main reason for these inadequacies is that the emphasis of ionisation calculations has been on the treatment of the electrons in the asymptotic region without special regard for the structure of the target ion. For highly ionised systems the effects of configuration interaction are important (Eissner and Nussbaumer 1969) and its inclusion has led to large changes in radiative transition probabilities and photoionisation cross sections (Pradhan 1980), for which no question

arises concerning the validity of any dynamical approximation such as the Coulomb–Born method or of exchange with an incident or scattered electron.

In this paper we will describe a method of calculating ionisation cross sections of complex positive ions, within the Coulomb–Born approximation (Jakubowicz and Moores 1980), using close-coupling wavefunctions to describe the states of the $(N+1)$-electron target ion and the N-electron residual ion plus ejected electron. The close-coupling method is capable of producing accurate wavefunctions both in the case of bound states and for continuum states when the energy of the free electron is small. Close-coupling wavefunctions are therefore particularly appropriate for the ionisation process since it is known that the ejected electron moves much more slowly than the ionising electron in the majority of ionisation events for incident electron energies away from threshold. This form of Coulomb–Born approximation does not suffer from any of the drawbacks discussed above and inner-shell ionisation, simultaneous excitation and ionisation together with autoionisation can all be accounted for directly in the calculation of the ionisation cross section by including appropriate N-electron target states in the close-coupling expansion. Furthermore, unless accurate target states are used to describe the $(N+1)$-electron system it is not possible to assess clearly the limitations inherent in the use of the Coulomb–Born approximation and the exchange approximations. Results will be presented for the beryllium-like ions C^{2+}, N^{3+}, O^{4+}, Ne^{6+}, Fe^{22+} and the lithium-like ions C^{3+}, N^{4+}, O^{5+} and Ne^{7+} including, for the first time, the effects of the autoionisation directly in the calculation of the cross sections for the lithium-like ions.

The following notation will be adopted. The ionising and ejected electrons will be labelled by $N+2$ and $N+1$ respectively and the space coordinates $\boldsymbol{r}_i$, and spin coordinates of the ith electron will be collectively denoted by $\boldsymbol{x}_i$. The states of both the target and residual ions will be described by orbital and spin angular momentum quantum numbers L, M_L, S, M_S with the other quantum numbers required to specify the states denoted by α. All quantities referring to states before (after) the collision will be identified by the subscript '0' ('γ') unless otherwise indicated. L–S coupling will be assumed to apply throughout, atomic units will be used in all the formulae and the phase convention of Edmonds (1960) will be used in the angular momentum algebra.

2. The Coulomb–Born approximation

If exchange between the ionising electron and the residual N-electron ion is neglected then the total cross section for ionisation is given by (Rudge 1969):

$$Q_\gamma = \int_0^{E_\gamma/2} \frac{k\chi_\gamma \, \mathrm{d}(\frac{1}{2}\chi_\gamma^2)}{4\pi k_0(2L_0+1)(2S_0+1)} \sum_{\substack{M_{S_0} M_{L_0} \\ M_{S_\gamma} M_{L_\gamma}}} \int \mathrm{d}\hat{k}_0 \, \mathrm{d}\hat{k} \, \mathrm{d}\hat{\chi}_\gamma$$
$$\times [|f(\boldsymbol{\chi}_\gamma, \boldsymbol{k})|^2 + |g(\boldsymbol{\chi}_\gamma, \boldsymbol{k})|^2 - \mathrm{Re}(f^*(\boldsymbol{\chi}_\gamma, \boldsymbol{k}) g(\boldsymbol{\chi}_\gamma, \boldsymbol{k}))] \tag{2.1}$$

where $\boldsymbol{k}_0$ ($\boldsymbol{k}$) is the momentum of the ionising electron before (after) the collision, $\boldsymbol{\chi}_\gamma$ is the momentum of the ejected electron, $f(\boldsymbol{\chi}_\gamma, \boldsymbol{k})$ the direct ionisation amplitude describing the ionisation process in which the electrons are assumed to be distinguishable, $g(\boldsymbol{\chi}_\gamma, \boldsymbol{k})$ is the exchange ionisation amplitude describing exchange in the continuum between electrons $N+1$ and $N+2$, and

$$E_\gamma = \tfrac{1}{2}k^2 + \tfrac{1}{2}\chi_\gamma^2 = \tfrac{1}{2}k_0^2 - I_\gamma \tag{2.2}$$

is the total energy of the continuum electrons with I_γ the ionisation energy for final state γ.

It is shown by Peterkop (1961) that f and g differ only in phase, i.e.

$$g(\boldsymbol{\chi}_\gamma, \boldsymbol{k}) = \exp(i\tau(\boldsymbol{\chi}_\gamma, \boldsymbol{k}))f(\boldsymbol{k}, \boldsymbol{\chi}_\gamma) \tag{2.3}$$

and that for exact amplitudes the phase difference $\tau(\boldsymbol{\chi}_\gamma, \boldsymbol{k})$ is uniquely defined. (Rudge and Seaton (1965) obtain the same result but use a phase convention in which $\tau(\boldsymbol{\chi}_\gamma, \boldsymbol{k})$ is zero when f and g are exact.)

The Coulomb–Born approximation to the direct amplitude is given by (Rudge and Schwartz 1966)

$$\begin{aligned} f_{CB}(\boldsymbol{\chi}_\gamma, \boldsymbol{k}) = -(2\pi)^{-5/2} \int \Psi_0^*(\alpha_0 S_0 L_0 M_{S_0} M_{L_0} | \boldsymbol{x}_1 \ldots \boldsymbol{x}_{N+1}) \\ \times \Big[\int \Big(\phi^*(Z-N-1, -\boldsymbol{k}_0 | \boldsymbol{x}_{N+2}) \\ \times \sum_{i=1}^{N+1} \frac{1}{r_{i,N+2}} \phi(Z-N-1, -\boldsymbol{k} | \boldsymbol{x}_{N+2}) \Big) \, d\boldsymbol{x}_{N+2} \Big] \\ \times \Psi_f(\boldsymbol{x}_1 \ldots \boldsymbol{x}_{N+1}) \, d\boldsymbol{x}_1 \ldots d\boldsymbol{x}_{N+1} \end{aligned} \tag{2.4}$$

where Z is the nuclear charge of the target ion, Ψ_0 is the ground-state eigenfunction of the $(N+1)$-electron Hamiltonian, H_{ion}, with energy E_0,

$$H_{\text{ion}}\Psi_0 = E_0\Psi_0 \tag{2.5}$$

and Ψ_f describes the state of the ejected electron plus residual ion and satisfies

$$H_{\text{ion}}\Psi_f = (E_{1\gamma} + \tfrac{1}{2}\chi_\gamma^2)\Psi_f \tag{2.6}$$

where $E_{1\gamma}$ is the energy of the residual ion. The functions $\phi(Z_i, -\boldsymbol{k}_i|\boldsymbol{x}_i)$ are Coulomb wavefunctions, defined in equation (3.1) below, for a charge Z_i, multiplied by a spin $-\frac{1}{2}$ eigenvector. In this work we will also consider the use of distorted Coulomb wavefunctions satisfying

$$H_{D,i}\phi = \tfrac{1}{2}k_i^2\phi \tag{2.7}$$

where

$$H_{D,i} = \tfrac{1}{2}\nabla_i^2 + \tfrac{1}{2}k_i^2 + Z_i/r_i + V(r_i) \tag{2.8}$$

and $V(r_i)$ are short-range potentials which are chosen so as to account for some of the distorting effect of the electrons around the ion and exchange with these electrons (see below).

When the Coulomb–Born approximation is used for the amplitudes, the condition

$$\frac{z_1}{k} + \frac{z_2}{\chi_\gamma} = \frac{Z}{k} + \frac{Z}{\chi_\gamma} - \frac{1}{|\boldsymbol{k} - \boldsymbol{\chi}_\gamma|}$$

(Rudge and Seaton 1965, Peterkop 1977, Rudge and Schwartz 1966) which expresses the asymptotic charges experienced by the electrons as a function of their momenta and of the angle between them, and which must be satisfied in order to take full account of the long-range Coulomb potentials, is not met. This implies (Peterkop 1977 ch 6) that the phase factor $\tau(\boldsymbol{\chi}_\gamma, \boldsymbol{k})$ in (2.3) is essentially arbitrary, so that some choice must be made for it. We will give results in three distinct exchange approximations: the

Coulomb–Born approximation (CB), the Coulomb–Born no exchange approximation (CBNX) and the Coulomb–Born exchange approximation (CBX).

In the Coulomb–Born approximation (CB), which is also sometimes referred to as the 'full range' Coulomb–Born approximation, exchange is ignored from the outset and the two continuum electrons are treated as being distinguishable. This results in the following expression for the total cross section:

$$Q_{\mathrm{CB}} = \int_0^{E_\gamma} \frac{k\chi_\gamma \, \mathrm{d}(\frac{1}{2}\chi_\gamma^2)}{4\pi k_0(2S_0+1)(2L_0+1)} \sum_{\substack{M_{S_0} M_{L_0} \\ M_{S_\gamma} M_{L_\gamma}}} \int \mathrm{d}\hat{\boldsymbol{k}} \, \mathrm{d}\hat{\boldsymbol{k}}_0 \, \mathrm{d}\hat{\boldsymbol{\chi}}_\gamma |f_{\mathrm{CB}}(\boldsymbol{\chi}_\gamma, \boldsymbol{k})|^2. \tag{2.9}$$

The integration over ejected-electron energies in equation (2.9) is over the complete energy range, but, because the magnitudes of the exchange and direct amplitudes are still given by equation (2.3), there is a contribution from events which can only occur by exchange and equation (2.9) is equivalent to

$$Q_{\mathrm{CB}} = \int_0^{E_\gamma/2} \frac{k\chi_\gamma \, \mathrm{d}(\frac{1}{2}\chi_\gamma^2)}{4\pi k_0(2L_0+1)(2S_0+1)} \sum_{\substack{M_{S_0} M_{L_0} \\ M_{S_\gamma} M_{L_\gamma}}} \int \mathrm{d}\hat{\boldsymbol{k}} \, \mathrm{d}\hat{\boldsymbol{k}}_0 \, \mathrm{d}\hat{\boldsymbol{\chi}}_\gamma (|f_{\mathrm{CB}}(\boldsymbol{\chi}_\gamma, \boldsymbol{k})|^2 + |g_{\mathrm{CB}}(\boldsymbol{\chi}_\gamma, \boldsymbol{k})|^2) \tag{2.10}$$

or

$$Q_{\mathrm{CB}} = Q_{\mathrm{CB,d}} + Q_{\mathrm{CB,e}} \tag{2.11}$$

where $Q_{\mathrm{CB,d}}$ and $Q_{\mathrm{CB,e}}$ are the first and second terms on the right-hand side of (2.10) respectively. Thus, although CB pretends to ignore exchange, it has a contribution from events which can occur by exchange alone.

In practice CB is found to severely overestimate the cross section and a better and more consistent approximation is obtained by putting the exchange terms equal to zero giving the Coulomb–Born no exchange approximation (CBNX)

$$Q_{\mathrm{CBNX}} = Q_{\mathrm{CB,d}}. \tag{2.12}$$

This is also equivalent to summing only over events in which the ejected electron is the slower. CBNX is also sometimes referred to as the 'half-range' Coulomb–Born approximation or the 'modified' Coulomb–Born approximation. Formally CBNX corresponds to the Coulomb–Born no exchange approximation for electron impact excitation of ions and is equivalent to putting the exchange amplitude equal to zero in equation (2.1). Whereas this is physically unsatisfactory the exchange and interference contributions tend to cancel each other and hence CBNX can be expected to give reliable estimates of cross sections. This is perhaps most easily understood by noting that the exchange amplitude attains its maximum value when it is identical to the direct amplitude, which is when the continuum electrons have equal velocities. In this case the exchange terms in equation (2.1) cancel and an expression corresponding to CBNX is obtained. CBNX also has the advantage of being relatively easy to calculate. The major problem with CBNX is that, because it does not completely account for the full range of possible electron energies, it does not correctly describe the thresholds for processes such as inner-shell excitation and autoionisation which lie above the energy required for ionisation of the ground state. These contribute at first only through the exchange amplitude in equation (2.1) and do not therefore appear in CBNX until twice their threshold energies. This point is of particular relevance in the case of ionisation of lithium-like ions (see below).

Attempts to evaluate equation (2.1) completely within the Coulomb–Born approximation are known as 'Coulomb–Born exchange' approximations (CBX) for which

$$Q_{\mathrm{CBX}} = Q_{\mathrm{CB,d}} + Q_{\mathrm{CB,e}} - Q_{\mathrm{CB,int}} \tag{2.13}$$

where

$$Q_{\mathrm{CB,int}} = \int_0^{E_\gamma/2} \frac{k\chi_\gamma \, \mathrm{d}(\frac{1}{2}\chi_\gamma^2)}{4\pi k_0(2S_0+1)(2L_0+1)} \sum_{\substack{M_{S_0}M_{L_0} \\ M_{S_\gamma}M_{L_\gamma}}} \int \mathrm{d}\hat{\boldsymbol{k}} \, \mathrm{d}\hat{\boldsymbol{k}}_0 \, \mathrm{d}\hat{\boldsymbol{\chi}}_\gamma \, \mathrm{Re}(f^*_{\mathrm{CB}}(\boldsymbol{\chi}_\gamma, \boldsymbol{k}) g_{\mathrm{CB}}(\boldsymbol{\chi}_\gamma, \boldsymbol{k})). \tag{2.14}$$

Using equation (2.3) the exchange amplitude can be written as

$$g_{\mathrm{CB}}(\boldsymbol{\chi}_\gamma, \boldsymbol{k}) = |f_{\mathrm{CB}}(\boldsymbol{k}, \boldsymbol{\chi}_\gamma)| \exp(\mathrm{i}\tau_{\mathrm{CB}}(\boldsymbol{\chi}_\gamma, \boldsymbol{k})). \tag{2.15}$$

In order to evaluate equation (2.1) in the Coulomb–Born approximation some choice must be made for τ_{CB}. In this work we adopt an approximation which is such that, in the limit of infinite nuclear charge, the interference term is a maximum. There is no rigorous justification for this or any other choice of phase, but as in the argument used above in the discussion of CBNX, it can be seen that exchange is most significant when the exchange and interference terms in the integrands in equation (2.1) cancel, which is precisely when the interference is a maximum. In addition, this form of CBX gives the correct result for the case of an infinitely charged nucleus and, because it sets a lower limit to the ionisation cross section, enables the importance of exchange to be assessed quantitatively by comparison with CB and CBNX results. Previous calculations which have used this type of approximation to the phase include those of Rudge and Schwartz (1966), Burgess and Rudge (1963) and Younger (1980a, b). Clearly CB and CBNX ionisation cross sections are automatically generated in the calculation of a CBX cross section.

All of the Coulomb–Born approximations, CB, CBNX and CBX, can be modified to allow for screening effects by using distorted Coulomb waves in place of Coulomb waves in equation (2.4) and these approximations will be distinguished by adding the prefix 'D' to the appropriate abbreviation.

3. The use of close-coupling wavefunctions in the Coulomb–Born approximation

In this section expressions will be derived for the total ionisation cross sections in the CB, CBNX and CBX approximations together with their distorted Coulomb wave counterparts using close-coupling wavefunctions to describe the states Ψ_0 and Ψ_f in the Coulomb–Born ionisation amplitude (equation (2.4)).

The Coulomb wavefunction or distorted Coulomb wavefunctions satisfying equation (2.7) can be expanded in partial waves as

$$\phi(z_i, -\boldsymbol{k}_i|\boldsymbol{x}_i) = \frac{4\pi}{k_i^{1/2} r_i} \sum_{lm} Y^*_{lm}(\hat{\boldsymbol{r}}_i) Y_{lm}(\hat{\boldsymbol{k}}_i) \mathrm{i}^{-l} \exp[\mathrm{i}(\sigma_l + \eta_l)] F_l(k_i, z_i, r_i) \delta(m_{s_i}|\boldsymbol{\sigma}) \tag{3.1}$$

where

$$\sigma_l = \arg \Gamma(l + 1 - \mathrm{i}z_i/k_i) \tag{3.2}$$

is the Coulomb phaseshift and η_l is a phaseshift which depends on the nature of the potentials $V_i(r_i)$ and is zero for the case of pure Coulomb waves. The functions

$F_l(k_i, z_i, r_i)$ are radial wavefunctions which are solutions of

$$\left(\frac{\mathrm{d}^2}{\mathrm{d}r^2}-\frac{l(l+1)}{r^2}+\frac{z_i}{r}+V(r)+k^2\right)F_l(k, z_i, r)=0 \tag{3.3}$$

with

$$F_l(k, z_i, 0)=0$$

$$F_l(k, z_i, r) \underset{r\to\infty}{\sim} k^{-1/2}\sin(\xi+\eta_l)$$

where

$$\xi = kr-\tfrac{1}{2}l\pi+(z_i/k)\ln 2kr+\sigma_l.$$

In this work the potentials $V_i(r_i)$, when used, are chosen to be Thomas–Fermi–Dirac–Amaldi statistical model potentials (Eissner and Nussbaumer 1969). Defining the total potential V_{TOT} as

$$V_{\mathrm{TOT}}(r)=Z/r+V(r) \tag{3.4}$$

then the statistical model potential is such that

$$V_{\mathrm{TOT}}(r)=\begin{cases}\dfrac{Z}{r} & r\to 0\\[2ex] \dfrac{Z-N-1}{r} & r\to\infty.\end{cases} \tag{3.5}$$

The short-range part of the potential accounts for the distortion of the electron wavefunction close to the ion due to the distribution of the $N+1$ electrons around the ion, which is assumed to be spherically symmetric, together with the possibility of exchange with the electrons in a static exchange approximation. Further details of the exact form of the potential used can be found in Eissner and Nussbaumer (1969).

The $(N+1)$-electron system both before and after the ionising collision will be described by close-coupling wavefunctions of the form discussed by Seaton (1974) and Jones (1974) and are calculated using the program IMPACT (Crees *et al* 1978). The initial state function Ψ_0 is given by

$$\Psi_0(\alpha_0 S_0 L_0 M_{S_0} M_{L_0}\pi|\boldsymbol{x}_1 \ldots \boldsymbol{x}_{N+1})=\sum_{i=1}^{N_c}\Theta_i+\sum_{j=1}^{N_b}c_j\Phi_j \tag{3.6}$$

(the symbol π refers to the parity). This is a linear combination of N_c free channel functions Θ_i, which are antisymmetrised vector-coupled products of N-electron wavefunctions (which may contain configuration interaction) and one-electron functions $\theta_i(\boldsymbol{x}_k)$, together with N_b bound channel functions Φ_j which are $(N+1)$-electron single-configuration bound-state functions constructed from the N-electron orbitals. The bound channels are introduced in order to satisfy orthogonality requirements (Burke and Seaton 1971) but also allow short-range correlation effects to be accounted for. Their inclusion is of particular importance in the present context since they enable configuration mixing (and in the case of the final state, autoionisation) to be included even in a single free channel approximation. If the Coulomb–Born excitation amplitude were being calculated rather than the Coulomb–Born ionisation amplitude, the wavefunctions Ψ_f would also be of the form of (3.6). In the case of ionisation, however,

the final state of the $(N+1)$-electron system is not a stationary state but is represented by

$$\Psi_f(\boldsymbol{x}_1 \ldots \boldsymbol{x}_{N+1})$$

$$= \sum_{\substack{LSM_LM_S \\ l_\gamma m_\gamma m_{S_\gamma}}} (-1)^{l_\gamma - L_\gamma - M_L + \frac{1}{2} - S_\gamma - M_S} \frac{2\pi}{\chi_\gamma^{1/2}} \mathrm{i}^{l_\gamma + 1} Y^*_{l_\gamma m_\gamma}(\hat{\boldsymbol{\chi}}_\gamma)$$

$$\times [(2L+1)(2S+1)]^{1/2} \begin{pmatrix} L_\gamma & l_\gamma & L \\ M_\gamma & m_\gamma & -M_L \end{pmatrix} \begin{pmatrix} S_\gamma & \frac{1}{2} & S \\ M_{S_\gamma} & m_{S_\gamma} & -M_S \end{pmatrix}$$

$$\times \Psi_\gamma(\alpha_\gamma SLM_S M_L \pi \,|\, \boldsymbol{x}_1 \ldots \boldsymbol{x}_{N+1}) \tag{3.7}$$

where the wavefunctions Ψ_γ are of the form of (3.6) and satisfy S-matrix boundary conditions. The sums over quantum numbers with subscripts γ imply a sum over all channels which are open at the energy considered for each L, S and π, which in turn implies a sum over all linearly independent solutions Ψ_γ for each $LS\pi$. It is convenient to regard the functions Ψ_0 and Ψ_γ as solution vectors of dimension $N_c + N_b$ with components defined by the individual terms in (3.6). The dimensionality of the solution vectors is then a function of LS and π and depends on the states of the N-electron target which are used to generate the free channels. Since we are interested in cross sections for a fixed initial electron energy and final state it is only necessary to include in (3.7) those linearly independent solutions corresponding to outgoing waves in channels for which the residual ion is in a state with energy E_γ. The other linearly independent solutions, corresponding to different states with energy $E_{\gamma'}$, contribute to a different cross section to that which is required and so need not be considered. The omitted column vector solutions could be used if desired to calculate cross sections for processes in which the system is left in state γ', corresponding to a different ejected-electron energy.

The asymptotic form of the one-electron radial functions associated with Ψ_γ, $F_{j\gamma}(\mathbf{S}\,|\,r)$ is for open channels j, γ

$$F_{j\gamma}(\mathbf{S}\,|\,r) \underset{r\to\infty}{\sim} \chi_j^{-1/2}[\exp(-\mathrm{i}\xi_j)\delta_{j\gamma} - \exp(\mathrm{i}\xi_j)S_{j\gamma}] \tag{3.8}$$

where $\mathbf{S}$ is the scattering matrix. The program IMPACT computes real wavefunctions $F_{j\gamma}(\mathbf{A}, \mathbf{B}\,|\,r)$ with asymptotic form (for open channels)

$$F_{j\gamma}(\mathbf{A}, \mathbf{B}\,|\,r) \underset{r\to\infty}{\sim} \chi_j^{-1/2}(\sin\xi_j A_{j\gamma} + \cos\xi_j B_{j\gamma}). \tag{3.9}$$

These are linear combinations of the $F_{j\gamma}(\mathbf{S}\,|\,r)$ to which they are related by the matrix transformation

$$\mathbf{F}(\mathbf{S}\,|\,r) = \mathbf{F}(\mathbf{A}, \mathbf{B}\,|\,r)\mathbf{X} \tag{3.10}$$

where

$$\mathbf{X} = -2\mathrm{i}(\mathbf{A} - \mathrm{i}\mathbf{B})^{-1}. \tag{3.11}$$

The corresponding functions $\Psi_\gamma(SLM_sM_L\pi\,|\,\mathbf{S})$ are then related to the functions $\Psi_\beta(SLM_sM_L\pi\,|\,\mathbf{A}, \mathbf{B})$ by the transformation

$$\Psi_\gamma(\mathbf{S}) = \sum_\beta \Psi_\beta(\mathbf{A}, \mathbf{B})X_{\beta\gamma}. \tag{3.12}$$

The sum over β in (3.12) is over the number of open channels corresponding to $SL\pi$.

We expand the inter-electronic potentials in the form

$$\sum_{i=1}^{N+1} \frac{1}{r_{i,N+2}} = \sum_{i=1}^{N+1} \sum_{\lambda,\mu} \frac{4\pi}{2\lambda+1} Y^*_{\lambda\mu}(\hat{\boldsymbol{r}}_i) Y_{\lambda\mu}(\hat{\boldsymbol{r}}_{N+2}) \frac{r_<^\lambda}{r_>^{\lambda+1}} \tag{3.13}$$

where $r_<$ ($r_>$) is the lesser (greater) of r_i and r_{N+2}.

In order to reduce the expression for the cross section to a form amenable to computation, we substitute (3.1), (3.13) and (3.7) in (2.4). The wavefunctions are then transformed to the total angular momentum representation $L^{\mathrm{T}}M_L^{\mathrm{T}}S^{\mathrm{T}}M_S^{\mathrm{T}}$. After some algebra, using the Wigner–Eckart theorem (Edmonds 1960) and carrying out the integrations and summations over the spin and angle variables, we obtain

$$Q_{\mathrm{CB,d}} = \int_0^{E_\gamma/2} \frac{8\,\mathrm{d}(\frac{1}{2}\chi_\gamma^2)}{k_0^2(2L_0+1)} \sum_{\substack{l_0 l_1 l_\gamma \\ L\lambda}} \frac{(2l_0+1)(2l_1+1)}{2\lambda+1} \begin{pmatrix} l_0 & \lambda & l_1 \\ 0 & 0 & 0 \end{pmatrix}^2$$
$$\times |\langle \alpha_0 S_0 L_0 \| T^\lambda(l_0 l_1 k_0 k) \| L S_0 \gamma(\chi_\gamma)\rangle|. \tag{3.14}$$

In (3.14) the notation $\langle \alpha_0 L_0 S_0 \| T^\lambda(l_0 l_1 k_0 k) \| L S_0 \gamma(\chi_\gamma)\rangle$ is used to represent the reduced matrix elements of an irreducible tensor operator with components

$$T^\lambda_\mu(l_0 l_1 k_0 k)|\boldsymbol{r}_1 \ldots \boldsymbol{r}_{N+1})$$
$$= \left(\frac{4\pi}{2\lambda+1}\right)^{1/2} \int_0^\infty F_{l_0}(k_0, Z-N-1, r_{N+2})$$
$$\times \sum_{i=1}^{N+1} Y^*_{\lambda\mu}(\hat{\boldsymbol{r}}_i) \frac{r_<^\lambda}{r_>^{\lambda+1}} F_{l_1}(k, Z-N-1, r_{N+2}) \mathrm{d}_{N+2}. \tag{3.15}$$

The notation γ (χ_γ) inside the ket is to signify that we are describing the process in which the ionised ion is left in state γ and an electron is ejected with energy χ_γ^2 Ryd. The reduced matrix elements can be further reduced to the form

$$\langle \alpha_0 S_0 L_0 \| T^\lambda \| L S_0 \gamma(\chi_0)\rangle$$
$$= \sum_{i_0 i_\gamma} (d_{i_0 i_\gamma}(F_{i_0}|F_{i_\gamma}) + e_{i_0 i_\gamma}(F_{i_0}|T^\lambda|F_{i_\gamma})) + \sum_{i_0 j_\gamma} v_{i_0 j_\gamma}(F_{i_0}|T^\lambda|P_{j_\gamma}) C_{j_\gamma}$$
$$+ \sum_{j_0 i_\gamma} c^\dagger_{j_0} v_{i_\gamma j_0}(P_{j_0}|T^\lambda|F_{i_\gamma}) + \sum_{j_0 j_\gamma} c^\dagger_{j_0} \tau^\lambda(l_0 l_1 k_0 k)_{j_0 j_\gamma} c_{j_\gamma} \tag{3.16}$$

where

$$\tau^\lambda(l_0 l_1 k_0 k) = \langle \Phi_{j_0} \| T^\lambda(l_0 l_1 k_0 k) \| \Phi_{j_\gamma}\rangle \tag{3.17}$$

and $P_j(r)$ are the radial parts of the wavefunctions of the N-electron system.

The quantities d_{ij}, e_{ij} and v_{ij} are algebraic coefficients computed by a program COBALG (Eissner and Moores 1980). It should be noted that the operators in equation (3.15) are functions of the incident and final energy of the ionising electron and must be evaluated before equation (3.16) can be applied. This is different from the case of photoionisation for which the operator is known and is independent of energy. The operators are, however, slowly varying and to a good approximation can be regarded as being constant over small ranges of energy; this is of particular importance when considering the analytic properties of the reduced matrix elements (see § 4). Using equation (2.15) we obtain an expression for $Q_{\mathrm{CB,e}}$ which is the same as (3.14) but with χ_γ replaced by k in the ket. The interference term, $Q_{\mathrm{CB,int}}$, given by equation (2.14) can

also be evaluated once the relative phase of the direct and exchange amplitudes has been approximated. Following Rudge and Schwartz (1966) we choose τ_{CB} such that in the expression for the cross section there is no dependence on the phase factors σ_l, η_l in the partial-wave expansion of the cross section.

In this approximation

$$Q_{CB,int} = \int_0^{E_\gamma/2} \frac{8\,d(\frac{1}{2}\chi_\gamma^2)}{k_0^2(2L_0+1)} \sum_{\substack{l_0 l_1 l_\gamma \\ LL'\lambda\lambda'}} (-1)^{L+L'+l_1+l_\gamma}(2l_0+1)$$

$$\times[(2L+1)(2L'+1)(2l_1+1)(2l_\gamma+1)]^{1/2}\begin{pmatrix} l_0 & \lambda & l_1 \\ 0 & 0 & 0 \end{pmatrix}\begin{pmatrix} l_0 & \lambda' & l_\gamma \\ 0 & 0 & 0 \end{pmatrix}$$

$$\times\begin{Bmatrix} L' & L_0 & \lambda' \\ l_1 & \lambda & l_0 \\ L_\gamma & L & l_\gamma \end{Bmatrix}\langle\alpha_0 L_0 S_0\|T^\lambda(l_1 l_0 k_0 \chi_\gamma)\|LS_0\gamma(k)\rangle$$

$$\times\langle L'S_0\gamma(\chi_\gamma)\|T^{\lambda'}(l_0 l_\gamma k_0 k)\|\alpha_0 L_0 S_0\rangle. \tag{3.18}$$

In the Coulomb–Born case it follows from the definition of σ_l, (3.2), that with this choice of phase, for Z_i sufficiently large, the interference terms will combine in such a way that the interference will be a maximum. The same applies to the distorted-wave case, in which for large Z_i the phaseshifts $\eta_l \ll \sigma_l$.

Equations (3.14), (3.16) and (3.18) are the results which are required for the calculation of ionisation cross sections in the CB, CBNX and CBX approximations and their distorted-wave counterparts. A general computer program, COBION, similar in structure to the program PHOTUC for the calculation of photoionisation cross sections (Saraph 1981), has been written to evaluate these expressions. In practice the close-coupling wavefunctions are calculated at fixed values of χ_γ and k for a given k_0 and hence the integral over ejected-electron energies can be evaluated only when the integrand has been evaluated at a sufficient number of energies. Because of the expense of calculating even a single point on the integration mesh, which requires the inclusion of sufficient total angular momenta L and S and partial waves to bring the integrals to convergence, an efficient means of integrating must be devised. In this work we have chosen to use an N-point Gaussian quadrature to evaluate the integral when the integrand is slowly and smoothly varying. This is equivalent to fitting the integrand to a $(2N+1)$-order polynomial but only requires N values of the integrand. At low energies (three times the ionisation energy) a three-point Gaussian was found to be sufficient while at the highest energies a six-point Gaussian was used. This ensures that the resulting cross sections are in error by no more than 2% through the use of this numerical integration. This is not important since the input data to IMPACT are chosen so as to give final accuracy of around this amount.

When autoionisation structure appears in the differential cross section the Gaussian method is no longer appropriate. Because of the expense of these calculations it is not practical to map out the structure in detail and hence it is useful to employ analytical techniques which enable the structure to be calculated with a minimum of effort and cost. The general technique for doing this in the multi-channel case for the ionisation problem has been described by Jakubowicz (1980) and is simply an extension of the application of quantum defect theory in the calculation of structures in photoionisation cross sections (Dubau and Wells 1973, Pradhan and Seaton 1981). Because the results given here are obtained using only single-channel wavefunctions, for which the more

general theory is not required, we will now describe a simple method for calculating the autoionisation effects, which in this case are due to the mixing of the open and bound channels rather than the mixing of open and closed channels.

4. Autoionisation

In order to describe the behaviour of the ionisation cross section when autoionisation is present it is necessary to consider the analytic behaviour of the reduced matrix elements

$$\langle \alpha_0 L_0 S_0 \| T^\lambda \| L S_0 \gamma(\chi_\gamma) \rangle \tag{4.1}$$

as a function of the ejected-electron energy. When multichannel close-coupling wavefunctions are used this problem is computationally much more involved than the equivalent problem in photoionisation because the operator T^λ is a function of the incident electron energy and is also a (slowly varying) function of the ejected-electron energy. Fortunately, the variation in the T^λ term due to the different ejected-electron energies, which manifests itself through the conservation of energy (equation (2.2)) can be neglected over short ranges of energy and the dominant energy variation arises from the resonant behaviour of the continuum close-coupling wavefunctions. The analytic development must, however, be carried out separately for each incident energy and, because partial-wave expressions are used, separately for each combination of partial waves contributing to a given resonant channel. Wavefunctions with values of $SL\pi$ which are not resonant can be treated as constant in the resonance region.

For single-channel wavefunctions equation (3.6) becomes

$$\Psi = \Theta + \sum_{j=1}^{N_b} c_j \Phi_j \tag{4.2}$$

and any resonant behaviour results from the mixing of the free channel and the bound channels. Since, by definition, the bound channel wavefunctions Φ_j are held constant, a considerable simplification is possible, the mixing manifesting itself in the variation of the coefficients c_j and the free channel Θ only. Since the matrix elements of equation (4.1) become

$$\langle \alpha_0 L_0 S_0 \| T^\lambda \| L S_0 \gamma(\chi_\gamma) \rangle = \langle \alpha_0 L_0 S_0 \| T^\lambda \| \Theta \rangle + \sum_j \langle \alpha_0 L_0 S_0 \| T^\lambda \| \Phi_j \rangle c_j \tag{4.3}$$

then, in order to obtain the analytic properties of the matrix element, it is only necessary to obtain the variation of the free-channel matrix elements and the coefficients c_j (the bound-channel matrix elements are assumed to be constant since the operators are slowly varying). It follows from quantum defect theory (Seaton 1978) that, if the wavefunction is normalised such that

$$F \underset{r\to\infty}{\sim} \sin \xi + \cos \xi R \tag{4.4}$$

where R is the reactance matrix and is a single number for the single-channel case, then in the free-channel matrix element, the coefficients c_j and R can be expanded in the form

$$\sum_{i=0}^{m} \alpha_i E^i + \sum_{j=1}^{n_{\text{pole}}} \frac{\beta_j}{E - E_j} \tag{4.5}$$

where α_i and β_i are constants. This equation expresses the fact that c_j and R, considered as functions of energy E, have n_{pole} poles, which occur at energies E_j, $j = 1$ to n_{pole}. The energies E_j correspond to the resonance positions.

If it is further assumed that the resonant behaviour is dominated by the bound-channel terms, since it is the bound channels which are causing the resonances, then a further simplification is possible because the resonant behaviour of all the matrix elements is determined by that of the coefficients c_j alone. This is equivalent to assuming that the coefficients β_j in an expansion of the free-channel matrix element in the form of equation (4.5) are much smaller than those for an expansion of the bound-channel terms in equation (4.3) and is valid for all the cases considered here. Thus, by fitting the coefficients c_j and $R = BA^{-1}$ to expressions of the form of equation (4.5), the energy variation of all the matrix elements in a given resonant channel is known at all incident energies and it is only necessary to calculate the matrix elements using wavefunctions normalised according to equation (4.4) at a single point close to the resonance for each incident energy required. Further discussion of this technique will be deferred until results are presented for lithium-like ions in § 6.

5. Results for beryllium-like ions

The results of the calculations of ionisation cross sections for the beyllium-like ions presented here are of the simplest kind because they do not include any effects due to autoionisation. The states which were included as close-coupling wavefunctions were of the form ^1L, with L taking values from zero to eight, and consisted simply of a single free channel of configuration $1s^2 2skl$ ($l = L$) except in the case of the ^1S where additional bound channels of configuration $1s^2 2s^2$, $1s^2 2s3s$ and $1s^2 3s^2$ were included. The bound channel of configuration $1s^2 3s^2$ does in fact give rise to autoionisation but its effect was found to be very small and it was consequently neglected. The ground-state wavefunction was of the same form as the ^1S continuum wavefunction. Partial waves up to $l = 17$ were included to describe the ionising electron. Since autoionisation is unimportant in this case, the Gaussian method was used to evaluate the complete integrals over ejected-electron energies. It is expected that the numerical accuracy is limited only by the use of the Gaussian method and should be better than 2%, particularly at the lower energies.

Results for the ions C^{2+}, N^{3+}, O^{4+}, Ne^{6+} and Fe^{22+} in the DCBX, CBX, DCBNX, CBNX, DCB and CB approximations are tabulated in tables 1–5 as a function of the reduced incident electron energy, X (obtained by dividing the incident electron energy by the calculated ionisation energy). The distorted-wave results for C^{2+}, N^{3+} and O^{4+} are also displayed in figures 1, 2 and 3 where they are compared with the available experimental data; to avoid confusion the calculations of other workers are not displayed. The general form of the results is the same in all cases. CB is not a good approximation and, as discussed in § 2, severely overestimates the cross section. CBNX appears to be quite adequate and in these cases is very similar to the results of the Lotz formula (L) (Lotz 1967). CBX, which is expected to be the best approximation in this group, yields results similar to those given by the infinite-Z method of Golden and Sampson (1977) (GS), indicating that the Golden and Sampson formula gives a reasonable approximation to the true Coulomb–Born exchange results for finite nuclear charge. The fact that the results of the two methods are virtually the same in the case of Fe^{22+} also indicates that the calculations are behaving correctly in the limit of a large nuclear charge (it should be

Table 1. Ionisation cross section (10^{-22} m^2) for C^{2+} (ionisation energy = 3.520 Ryd). X is the ratio of incident electron energy to the ionisation energy.

	This work[a]						Others		
X	DCBX	CBX	DCBNX	CBNX	DCB	CB	CBNX[b]	GS[c]	L[d]
1.125	3.19	4.20	2.94	3.16	5.41	5.92	—	3.82	4.11
1.25	5.58	7.03	5.38	5.63	9.34	9.99	5.36	6.28	7.01
1.50	8.64	10.39	8.96	9.12	14.23	14.83	8.67	9.09	10.61
2.00	11.38	12.90	12.59	12.60	17.85	18.18	—	11.13	13.60
2.25	—	—	—	—	—	—	12.66	11.40	14.15
2.50	12.23	13.42	13.82	13.77	18.32	18.47	—	11.44	14.39
3.00	12.33	13.26	14.04	13.97	17.76	17.82	13.16	11.16	14.38
4.00	11.64	12.22	13.25	13.16	15.79	15.79	—	10.16	13.61
4.50	11.21	11.68	12.71	12.62	14.84	14.79	11.88	9.64	12.64
5.00	10.75	11.13	12.13	12.04	13.93	13.87	—	9.14	12.64
6.00	—	—	—	—	—	—	10.28	8.26	11.72

[a] Ionisation energy calculated by IMPACT was 3.373 Ryd.
[b] Moores (1978).
[c] Moores *et al* (1980).
[d] Lotz (1968).

Table 2. Ionisation cross section (10^{-22} m^2) for N^{3+} (ionisation energy = 5.694 Ryd).

	This work[a]						Others		
X	DCBX	CBX	DCBNX	CBNX	DCB	CB	CBNX[b]	GS[c]	L[d]
1.125	1.35	1.57	1.26	1.29	2.34	2.41	—	1.52	1.57
1.25	2.31	2.63	2.25	2.28	3.95	4.04	2.11	2.51	2.68
1.50	3.48	3.87	3.64	3.66	5.82	5.91	3.37	3.63	4.05
2.00	4.51	4.85	4.99	4.98	7.12	7.17	—	4.45	5.20
2.25	—	—	—	—	—	—	4.83	4.55	5.40
3.00	4.85	5.05	5.52	5.50	6.98	6.98	4.98	4.46	5.49
4.00	4.52	4.64	5.15	5.12	6.13	6.12	—	4.06	5.20
4.50	—	—	—	—	—	—	4.47	3.85	5.01
5.00	4.22	4.30	4.77	4.73	5.46	5.42	—	3.65	4.83
6.00	—	—	—	—	—	—	3.86	3.30	4.48

[a] Ionisation energy calculated by IMPACT was 5.519 Ryd.
[b] Moores (1978).
[c] Moores *et al* (1980).
[d] Lotz (1968).

noted, however, that relativistic effects may be important for this ion, and are not included here). The differences between the CBNX results obtained here and those of Moores (1978) on C^{2+} and N^{3+} can only be due to the different approximations which are made from the target states (Moores uses distorted waves to describe the target). This emphasises the importance of using accurate target states for complex ions even though the states used here are not as accurate as might be desired (see below).

The effect of allowing for distortion and exchange in the wavefunctions describing the ionising electron before and after the collision by using the Thomas–Fermi–Dirac–

Table 3. Ionisation cross section (10^{-22} m^2) for O^{4+} (ionisation energy = 8.371 Ryd).

	This work[a]					Others		
X	DCBX	CBX	DCBNX	CBNX	DCB	CB	GS[b]	L[c]
1.125	0.66	0.72	0.61	0.62	1.14	1.16	0.72	0.73
1.25	1.11	1.20	1.08	1.09	1.90	1.93	1.19	1.24
1.50	1.67	1.78	1.73	1.74	2.78	2.80	1.88	1.87
2.00	2.13	2.23	2.35	2.35	3.36	3.38	2.11	2.40
3.00	2.24	2.31	2.55	2.57	3.24	3.26	2.12	2.54
4.00	2.10	2.18	2.40	2.44	2.85	2.90	1.93	2.40
5.00	1.93	1.99	2.18	2.22	2.50	2.53	1.74	2.23

[a] Ionisation energy calculated by IMPACT was 8.167 Ryd.
[b] Moores *et al* (1980).
[c] Lotz (1968).

Table 4. Ionisation cross section (10^{-22} m^2) for Ne^{6+} (ionisation energy = 15.234 Ryd).

	This work[a]					Others		
X	DCBX	CBX	DCBNX	CBNX	DCB	CB	GS[b]	L[c]
1.05	0.093	0.097	0.084	0.084	0.162	0.164	0.103	0.097
1.125	0.208	0.216	0.193	0.194	0.360	0.362	0.226	0.219
1.25	0.351	0.364	0.340	0.342	0.599	0.603	0.371	0.374
1.50	0.521	0.536	0.540	0.541	0.867	0.872	0.538	0.566
1.75	0.610	0.625	0.657	0.658	0.988	0.993	0.620	0.669
2.00	0.657	0.670	0.724	0.725	1.036	1.040	0.659	0.725
2.25	0.681	0.692	0.762	0.762	1.046	1.050	0.674	0.754
2.50	0.687	0.697	0.776	0.777	1.033	1.050	0.677	0.677
3.00	0.683	0.690	0.779	0.778	0.987	0.988	0.660	0.767
3.50	0.663	0.668	0.757	0.756	0.926	0.926	0.632	0.750
4.00	0.636	0.640	0.725	0.724	0.863	0.862	0.601	0.725
4.50	0.609	0.611	0.691	0.689	0.805	0.804	0.570	0.700
5.00	0.581	0.583	0.656	0.655	0.752	0.751	0.541	0.674

[a] Ionisation energy calculated by IMPACT was 14.966 Ryd.
[b] Moores *et al* (1980).
[c] Lotz (1968).

Table 5. Ionisation cross section (10^{-25} m^2) for Fe^{22+} (ionisation energy calculated by IMPACT to be 141.4 Ryd. X, GS and L as previously.

	This work					Others		
X	DCBX	CBX	DCBNX	CBNX	DCB	CB	GS	L
1.125	2.64	2.63	2.38	2.38	4.43	4.43	2.79	2.55
1.25	4.40	4.38	4.15	4.15	7.30	7.31	4.52	4.34
1.50	6.44	6.40	6.48	6.49	10.44	10.45	6.55	6.58
2.00	7.91	7.88	8.54	8.54	12.25	12.26	8.02	8.48
3.00	8.00	7.96	9.00	8.99	11.42	11.42	8.04	8.91
4.00	7.34	7.31	8.29	8.28	9.88	9.86	7.32	8.43
5.00	6.66	6.63	7.47	7.45	8.56	8.54	6.59	7.83

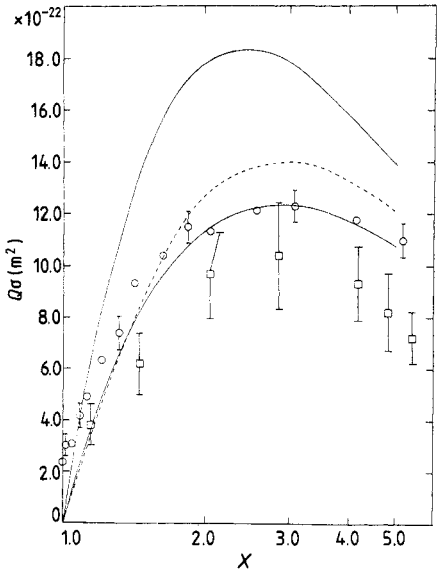

Figure 1. Ionisation cross section of C^{2+}. – – –, DCBNX; —— (upper), DCB; —— (lower), DCBX. The circles are the crossed-beam data of Woodruff *et al* (1978) and the squares are trapped-ion data of Hamdan *et al* (1978). The ordinate X is the ratio of incident electron energy to the ionisation energy.

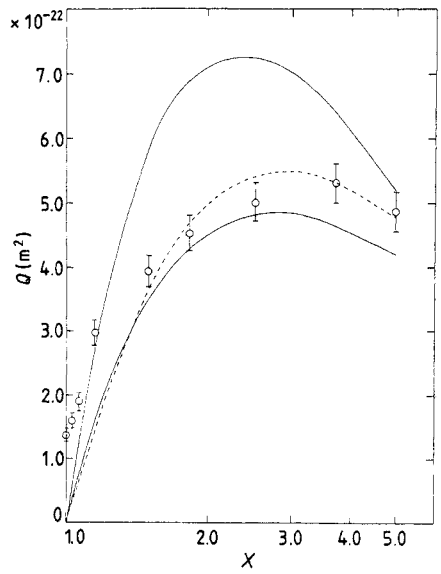

Figure 2. Ionisation cross section of N^{3+}. – – –, DCBNX; —— (upper), DCB; —— (lower), DCBX. The experimental points are the crossed-beam data of Crandall *et al* (1979).

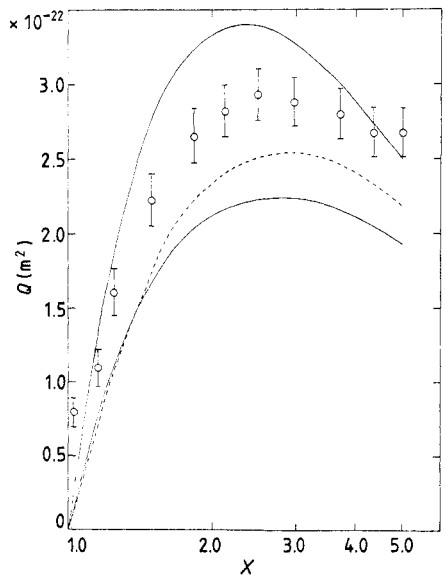

Figure 3. Ionisation cross section of O^{4+}. – – –, DCBNX; —— (upper), DCB; —— (lower), DCBX. The experimental points are the crossed-beam data of Crandall *et al* (1979).

Amaldi statistical model potential is to decrease the cross section from its undistorted value in all cases. The effect is most marked for the lower charged ions and at low energies where it is expected that the effect of the interelectronic potentials in the total Hamiltonian of the system is relatively more important. This is most pronounced in the

exchange and interference terms since these include wavefunctions which describe the ionising electron as moving more slowly than the ejected electron. In particular, the interference term is affected most of all because the reduction in magnitude of the exchange amplitude is magnified by the larger direct amplitude. This accounts for the fact that the DCBX and CBX results differ from each other by much more than either the DCBNX and CBNX or the DCB and CB results. The effect of distortion decreases with increasing charge as expected, and for Ne^{6+} there is very little difference between the DCBX and CBX results. The small differences in the distorted-wave and Coulomb-wave results for Fe^{22+} are purely numerical in origin. These conclusions are also borne out by the results of Younger (1980a) on He- and Li-like ions.

A measure of the quality of the close-coupling wavefunctions can be gained by comparing the value of the ionisation energy calculated by IMPACT with the experimental value. In all cases the calculated value is lower than the observed value because the state of the three-electron ion ($1s^2 2s\ ^2S$) which is coupled to the extra electron to generate the wavefunction has an artificially high energy in the single-state approximation. This means that configuration mixing, in this case predominantly from the $1s^2 2p^2\ ^1S$ state, which has been neglected in these calculations is important for these systems and the $1s^2 2p\ ^2P$ configuration should be included to generate accurate wavefunctions. This has not been attempted for the present because of the complexity of treating the resonances resulting from the mixing of the channels when the higher channel is closed.

The comparison with experimental data is complicated by the fact that in all cases the absolute crossed-beam data (Woodruff *et al* (1978) for C^{2+} and Crandall *et al* (1979) for N^{3+} and O^{4+}) were obtained using beams contaminated with metastable components consisting of $1s^2 2s2p\ ^3P$ states which contribute to the measured cross sections in unknown amounts; this accounts for the finite values of the measured cross sections at threshold. In their experiments with the Be-like ions N^{3+} and O^{4+} Crandall *et al* estimated the fraction of ions initially in the ^3P metastable state to be about 50%. When comparison is made between their measurements and with theoretical results calculated for a 50–50 mixture of ground and metastable states, they obtain best agreement with the Lotz formula (within 10%). Away from threshold the metastable contributions should however be less important, although without rigorous measurements or calculations of the cross sections it is not possible to say with certainty whether this is the case. With this *caveat*, it appears that the results which have the soundest foundation in theory, DCBX, give an excellent representation of the crossed-beam data for C^{2+} above about twice the threshold for ionisation of the ground state, where the metastable contribution should have ceased to be important. For N^{3+} and O^{4+} the agreement becomes progressively worse and it appears that DCBNX (or CBNX) and Lotz's method give the best agreement. This is disturbing because the DCBX results are expected to improve with increasing charge of the target and because the experimental cross sections are not scaling as theory would predict. (It should be noted that the Lotz formula depends on the scaling for its validity). It is not possible at present to resolve these discrepancies and further theoretical and experimental work is required on these ions. The most obvious shortcoming of the results presented here is the neglect of configuration interaction in the close-coupling wavefunction. On the other hand, although the trapped-ion measurement of Hamdan *et al* (1978) is not absolute and must also be viewed with caution, it does not have any metastable contribution and may indicate that, for C^{2+} at least, the crossed-beam results are too high.

For ionisation balance calculations, the important quantity is the rate coefficient $\alpha(T)$ defined by

$$\alpha(T) = 5.465 \times 10^{-17} T^{1/2} \int_{U_0}^{\infty} Q(UkT) U \exp(-U)\, \mathrm{d}U \quad \mathrm{m^3\ s^{-1}} \tag{5.1}$$

where $U = \frac{1}{2}k_0^2/kT$ and Q is in m^2. In table 6 we compare the results obtained by substituting our best cross section results (DCBX) in equation (5.1) with the Lotz formula

$$\alpha(T) = 3 \times 10^{-12} \frac{I_{nl}}{I_\gamma (kT)^{1/2}} E_1(I_\gamma/kT) \tag{5.2}$$

where $E_p(x)$ is the exponential integral of order p and r_{nl} is the number of electrons in the shell which is being ionised. Also shown are results obtained from the infinite-Z approximation as revised by Moores *et al* (1980)

$$\begin{aligned}\alpha(T) = \pi a_0^2 \left(\frac{8hT}{\pi m_e}\right)^{1/2} \left(\frac{I_H}{kT}\right) \frac{n^2 r_{nl}}{Z_{\mathrm{eff}}^2} \\ \times \{D'' \exp(-y) + [A'' + y(c'' - 2D'')] E_1(y) \\ + y(D'' + d'' - c'') E_2(y) - d'' y E_3(y)\}\end{aligned} \tag{5.3}$$

where n is the principal quantum number of the initial state, $y = I_\gamma/kT$ and the coefficients Z_{eff}, A'', D'', c'' and d'' are tabulated by Moores *et al* (1980).

It can be seen from table 6 that the Lotz formula gives larger ionisation rates than the present results, but the difference is never more than 25%, except for the case of Fe^{22+} above 10^8 K, where the Lotz formula is up to 50% higher. In all cases the difference between Lotz and the present results is largest at the higher temperatures where the main contribution to the rate coefficient comes from the high-energy part of the cross section. This is particularly the case in Fe^{22+}. Our calculated cross sections have been extrapolated to higher energies by fitting to the cross sections of Moores *et al* (1980), which should be more accurate than the simple Lotz formula at high energies.

The rate coefficients obtained from equation (5.3) are in good agreement with our results, especially at low temperatures. The difference is less than 15% in all cases. All the rate coefficients tabulated include contributions, calculated from (5.3), from inner-shell (1s) ionisation which is non-negligible above 2×10^6 K.

6. Results for lithium-like ions

Results for the lithium-like ions C^{3+}, N^{4+}, O^{5+} and Ne^{7+} are given in tables 7–10 and the undistorted Coulomb wave results for C^{3+}, N^{4+} and O^{5+} are plotted together with the experimental data of Crandall *et al* (1979) in figures 4, 5 and 6 respectively. These results were obtained using close-coupling wavefunctions of the form ^2L with L taking values from zero to eight which were formed by coupling the configuration $1s^2$ to the added electron to give a single free channel of configuration $1s^2kl$ ($l = L$) together with bound channels of configuration $1s^22s$, $1s2s^2$, $1s2p^2$, $2s2p^2$ in the ^2S state and $1s^22p$, $1s2s(^1S)2p$, $1s2s(^3S)2p$, $2s^22p$, $2p^3$ in the ^2P state. All of the bound channels except the $1s^22s$ and $1s^22p$ states give rise to autoionisation but the states $2s2p^2$, $2s^22p$ and $2p^3$ do not contribute at the energies of interest here. The ground-state wavefunctions were of the same form as the ^2S continuum states. The autoionisation can be seen as large

Table 6. Ionisation rate coefficients for Be-like ions.

	C^{2+}			N^{3+}		
T (K)	JM	MGS	L	JM	MGS	L
2×10^5	0.427	0.450	0.524	0.033	0.036	0.039
4	2.11	2.08	2.53	0.398	0.408	0.461
6	3.65	3.47	4.34	0.940	0.934	1.08
1×10^6	5.65	5.16	6.72	1.90	1.82	2.18
2	7.59	6.70	9.27	3.19	2.93	3.72
4	8.22	7.13	10.6	3.98	3.55	4.79
6	8.08	6.98	10.8	4.12	3.64	5.12
1×10^7	7.54	6.50	10.6	4.06	3.57	5.27
2	6.48	5.59	9.69	3.66	3.21	5.08
5	4.96	4.29	8.07	2.92	2.57	4.40
1×10^8	3.87	3.39	6.76	2.35	2.07	3.77
	O^{4+}			Ne^{6+}		
T (K)	JM	MGS	L	JM	MGS	L
2×10^5	0.002	0.002	0.002	0.	0.	0.
4	0.071	0.075	0.080	0.002	0.002	0.002
6	0.241	0.247	0.272	0.014	0.015	0.015
1×10^6	0.659	0.655	0.744	0.081	0.083	0.088
2	1.42	1.36	1.62	0.315	0.315	0.348
4	2.03	1.89	2.40	0.627	0.609	0.710
6	2.24	2.06	2.71	0.780	0.748	0.903
1×10^7	2.32	2.12	2.93	0.906	0.860	1.09
2	2.20	1.90	2.96	0.953	0.899	1.21
5	1.82	1.66	2.67	0.860	0.809	1.19
1×10^8	1.50	1.37	2.34	0.734	0.690	1.09
	Fe^{22+}					
T (K)	JM	MGS	L			
6×10^6	0.001	0.001	0.001			
1×10^7	0.004	0.004	0.004			
2	0.013	0.013	0.014			
5	0.026	0.026	0.030			
1×10^8	0.031	0.031	0.038			
2	0.034	0.034	0.044			
4	0.032	0.032	0.044			
6	0.030	0.029	0.042			
8	0.028	0.028	0.040			
1×10^9	0.026	0.026	0.039			

JM: present results.
MGS: Moores *et al* (1980).
L: Lotz (1968).
E: Crandall *et al* (1979).
SG: Sampson and Golden (1979).

Table 7. Ionisation cross section (10^{-22} m^2) for C^{3+} (ionisation energy = 4.740 Ryd).

	This work[a]						Others			
X	DCBX	CBX	DCBNX	CBNX	DCB	CB	CBNX[b]	GS[c]	GS[d]	L
1.05	0.42	0.46	0.37	0.39	0.73	0.75	—	0.49	0.49	0.50
1.125	0.94	1.01	0.87	0.89	1.61	1.67	—	1.08	1.08	1.13
1.25	1.58	1.69	1.54	1.58	2.70	2.78	1.49	1.77	1.77	1.93
1.50	2.35	2.49	2.46	2.50	3.95	4.04	2.35	2.57	2.57	2.92
1.75	2.76	2.90	3.01	3.05	4.52	4.62	—	2.96	2.96	3.46
2.00	2.98	3.11	3.33	3.37	4.77	4.82	—	3.15	3.15	3.75
2.25	3.09	3.21	3.51	3.54	4.82	4.90	3.33	3.22	3.22	3.90
2.50	3.14	3.24	3.59	3.62	4.79	4.86	—	3.23	3.23	3.97
2.75	3.14	3.24	3.61	3.64	4.69	4.75	—	3.20	3.20	3.98
3.00	3.12	3.20	3.60	3.67	4.57	4.62	3.40	3.15	3.15	3.96
3.25	3.11	3.16	3.56	3.58	4.43	4.48	—	3.09	3.09	3.92
3.50	3.03	3.10	3.50	3.52	4.29	4.33	—	3.02	3.02	3.87
3.75	2.98	3.04	3.43	3.45	4.15	4.19	—	2.95	2.95	3.81
4.00	2.91	2.97	3.35	3.37	4.00	4.03	3.18	2.87	2.87	3.75
4.25	2.85	2.90	3.27	3.28	3.86	3.89	—	2.80	2.80	3.68
4.50	2.79	2.83	3.19	3.20	3.73	3.75	—	2.72	2.72	3.62
4.75	—	3.16	—	3.17	—	4.02	—	2.65	3.08	3.55
5.00	—	3.08	—	3.08	—	3.89	—	2.58	2.99	3.48
5.25	—	3.00	—	2.99	—	3.76	—	2.52	2.91	3.42
6.00	—	—	—	—	—	—	2.60	2.33	2.84	3.23

[a] Ionisation energy calculated by IMPACT was 4.730 Ryd.
[b] Moores (1978).
[c] Without autoionisation.
[d] With autoionisation.

increases in the measured ionisation cross section and in the CBX and CB cross sections at about four times the ionisation threshold.

Below the autoionisation threshold the differential cross section is a slowly and smoothly varying function of the ejected-electron energy and the integration over the ejected-electron energies was performed using the Gaussian method. When the autoionisation threshold is crossed sharp peaks appear in the differential cross section as the flux increases through the mixing of the bound channels with the continuum. This is illustrated in figure 7 where the calculated differential cross section $\sigma(\chi^2)$ (defined such that $\int \sigma(\chi^2)\, d\chi^2 = Q_{CBX}$, where Q_{CBX} is given by (2.13)) for Ne^{7+} at the incident energy of about five times the ionisation energy is plotted as a function of the ejected-electron energy in the regions where the $1s2s^2\ ^2S$, $1s2s(^1S)2p\ ^2P$, $1s2s(^3S)2p\ ^2P$ states give rise to autoionisation. In the case of the $1s2s(^1S)2p\ ^2P$ state an increase of four orders of magnitude is found. The curves in figure 7 were generated using the technique described in § 5. The R matrices and c_j coefficients for the ^2S and ^2P channels were obtained at a series of energies about the resonances and fitted to expressions of the form of equation (6.1). The reduced matrices were then calculated at a point close to the resonance of interest and hence, using the known variation of the R matrix and c_j coefficients, the structures could be generated. In the case of figure 7, the $1s2s^2\ ^2S$ resonance was generated using data calculated at an energy $\chi_\gamma^2 = 48.5$ Ryd while both the ^2P structures were calculated using data calculated at $\chi_\gamma^2 = 49.5$ Ryd. It can be seen that the method accurately reproduces the peaks in the differential cross section both in

Table 8. Ionisation cross-section (10^{-22} m) for N^{4+} (ionisation energy = 7.195 Ryd).

	This work[a]						Others			
X	DCBX	CBX	DCBNX	CBNX	DCB	CB[a]	CBNX[b]	GS[c]	GS[d]	L
1.05	0.19	0.20	0.17	0.17	0.34	0.34	—	0.22	0.22	0.22
1.125	0.43	0.44	0.40	0.40	0.75	0.75	—	0.48	0.48	0.49
1.25	0.72	0.74	0.71	0.71	1.24	1.25	0.67	0.80	0.80	0.79
1.50	1.07	1.09	1.12	1.12	1.80	1.81	1.07	1.15	1.15	1.27
1.75	1.25	1.27	1.36	1.36	2.05	2.06	—	1.33	1.33	1.50
2.00	1.35	1.37	1.50	1.50	2.15	2.16	—	1.41	1.41	1.63
2.25	1.39	1.41	1.57	1.58	2.17	2.18	1.50	1.44	1.44	1.70
2.50	1.41	1.43	1.61	1.61	2.15	2.16	—	1.49	1.49	1.72
2.75	1.41	1.42	1.62	1.62	2.11	2.11	—	1.44	1.44	1.73
3.00	1.40	1.41	1.61	1.61	2.05	2.05	1.52	1.41	1.41	1.72
3.25	1.39	1.39	1.59	1.59	1.97	1.99	—	1.39	1.39	1.71
3.50	1.36	1.37	1.56	1.56	1.92	1.92	—	1.35	1.35	1.68
3.75	1.34	1.34	1.53	1.53	1.86	1.86	—	1.32	1.32	1.66
4.00	1.31	1.31	1.50	1.50	1.79	1.79	—	1.29	1.29	1.63
4.20	1.29	1.29	1.47	1.47	1.74	1.74	—	1.26	1.26	1.61
4.40	—	1.48	—	1.45	—	1.90	—	1.23	1.45	1.58
4.50	—	—	—	—	—	—	1.35	1.22	1.43	1.57
4.75	—	1.42	—	1.38	—	1.81	—	1.19	1.39	1.54
5.00	—	1.40	—	1.35	—	1.75	—	1.16	1.41	1.51
5.25	—	1.37	—	1.32	—	1.70	—	1.13	1.38	1.49
6.00	—	—	—	—	—	—	1.16	1.05	1.31	1.40

[a] Ionisation energy calculated by IMPACT was 7.181 Ryd.
[b] Moores (1978).
[c] Without autoionisation.
[d] With autoionisation.

height and shape. There are small discrepancies away from the resonances due to the neglect of variations in the contributions from the free channel terms, the non-resonant channels and the operators T^{λ}, none of which are taken into account. These discrepancies do not give rise to any significant errors when the integration over the differential cross section is carried out, in this case using the trapezoidal rule. The contributions to the integrals away from the resonances are calculated using the Gaussian method. Because the resonances only appear in the exchange amplitude at the energies of interest here, the CBNX results do not contain any contribution from the autoionisation and the continuity of the CBNX cross section across the threshold enables the accuracy of the numerical integration to be checked. This also indicates that it is a good approximation to assume that the direct amplitude is constant in the resonance region.

The general form of the results is the same in all cases. Below the autoionisation threshold one may draw conclusions similar to those made for the beryllium-like ions where no autoionisation is present. Again, CB is poor, CBNX is adequate and CBX is probably the best of the approximations. The effect of using distorted waves is less pronounced than in the case of the beryllium-like ions, partly because the charge on the target ion is higher in these cases and partly because there are fewer electrons in the ions. For O^{5+} and Ne^{7+} the effect of distortion is expected to be very small and hence distorted-wave calculations were not carried out for these ions. The DCBX and CBX

Table 9. Ionisation cross section (10^{-22} m^2) for O^{5+} (ionisation energy = 10.152 Ryd).

	This work[a]			Others						
X	CBX	CBNX	CB	DCBX[b]	CBX[b]	DCBNX[b]	CBNX[b]	GS[c]	GS[d]	L
1.05	0.099	0.089	0.173	—	—	—	—	0.113	0.113	0.110
1.125	0.221	0.205	0.382	0.220	0.210	0.215	0.211	0.248	0.248	0.247
1.25	0.371	0.361	0.635	0.367	0.369	0.361	0.370	0.408	0.408	0.421
1.50	0.550	0.571	0.920	0.542	0.580	0.543	0.580	0.590	0.590	0.638
	0.548[e]	0.567[e]	0.915[e]							
1.75	0.643	0.695	1.047	—	—	—	—	0.680	0.680	0.755
2.00	0.691	0.765	1.097	—	—	—	—	0.723	0.723	0.818
2.25	0.715	0.803	1.107	0.698	0.807	0.694	0.807	0.740	0.740	0.859
2.50	0.723	0.820	1.095	—	—	—	—	0.742	0.742	0.865
	0.714[e]	0.811[e]	1.086[e]							
2.75	0.722	0.824	1.071	—	—	—	—	0.736	0.736	0.868
3.00	0.716	0.819	1.041	—	—	—	—	0.725	0.725	0.864
3.25	0.706	0.809	1.008	—	—	—	—	0.710	0.710	0.856
3.50	0.698	0.799	0.978	—	—	—	—	0.694	0.694	0.845
3.98	0.668	0.763	0.912	—	—	—	—	0.661	0.661	0.819
4.14	0.773	0.760	1.006	—	—	—	—	0.650	0.773	0.810
4.25	0.768	0.752	0.997	—	—	—	—	0.643	0.763	0.803
4.50	0.758	0.729	0.968	—	—	—	—	0.626	0.741	0.789
4.75	0.737	0.711	0.933	—	—	—	—	0.609	0.749	0.774
5.00	0.719	0.690	0.901	—	—	—	—	0.594	0.733	0.760
5.25	0.712	0.672	0.874	—	—	—	—	0.578	0.722	0.745

[a] Ionisation energy calculated by IMPACT was 10.133 Ryd.
[b] Younger (1980a).
[c] Without autoionisation.
[d] With autoionisation.
[e] Five-state close-coupling results calculated ionisation energy was 10.211 Ryd.

results of Younger (1980a) on O^{5+}, which are similar to our own, and on Mg^{9+} confirm this. Similarly, at the high energies corresponding to the onset of autoionisation, distortion effects will be small and only Coulomb-wave results are presented.

Above the autoionisation threshold the dominant contributions to the cross sections are from the 'knockout' process and the autoionisation from the $1s2s(^1S)2p\ ^2P$ resonance. The other resonances contribute to a much smaller degree. As each resonance is crossed the total cross section should increase quasi-stepwise. No attempt has been made to map out this structure in these calculations and results are given immediately below the threshold of the $1s2s^2\ ^2S$ resonance and immediately above the threshold of the $1s2s(^3S)2p\ ^2P$ resonance (the $1s2p^2\ ^2S$ resonance lies still higher in energy but gives very little contribution to the cross section). The positions of the resonances as calculated by IMPACT are listed in table 11. These are in good agreement with the experimentally determined thresholds and the close-coupling results of Henry (1979) which do not, however, allow for mixing between the excited states and the continuum.

One of the assumptions which is implicit in the form of the close-coupling wavefunctions used in these calculations is that all the autoionising states only decay into the continuum and cannot decay by radiative emission. In order to correct for such effects within the framework of the present formulation it would be necessary to include

Table 10. Ionisation cross section (10^{-22} m^2) for Ne^{7+} (ionisation energy = 17.573 Ryd).

	This work[a]			Others		
X	CBX	CBNX	CB	GS[b]	GS[c]	L
1.05	0.035	0.031	0.061	0.039	0.039	0.037
1.125	0.077	0.072	0.134	0.085	0.085	0.082
1.25	0.129	0.126	0.222	0.140	0.140	0.141
1.50	0.191	0.198	0.320	0.202	0.202	0.213
1.75	0.222	0.240	0.362	0.233	0.233	0.252
2.00	0.238	0.263	0.378	0.248	0.248	0.273
2.25	0.245	0.276	0.381	0.254	0.254	0.284
2.50	0.247	0.281	0.376	0.254	0.254	0.289
2.75	0.245	0.280	0.366	0.252	0.252	0.290
3.00	0.244	0.280	0.356	0.248	0.248	0.288
3.25	0.240	0.276	0.344	0.243	0.243	0.286
3.50	0.236	0.271	0.332	0.238	0.238	0.282
3.72	0.232	0.266	0.322	0.233	0.233	0.278
3.84	0.276	0.264	0.363	0.230	0.278	0.276
4.50	0.267	0.246	0.331	0.214	0.268	0.263
5.00	0.249	0.233	0.311	0.203	0.259	0.253

[a] Ionisation energy calculated by IMPACT was 17.539 Ryd.
[b] Without autoionisation.
[c] With autoionisation.

radiative terms in the Hamiltonian (Davies and Seaton 1969), a procedure which could rapidly lead to the problem becoming numerically intractable. It is apparent, however, from the work of Gabriel (1972) on the autoionisation and radiative transition probabilities of the states considered here that the loss of flux from the ionisation process by radiative decay is only important for ions with nuclear charge greater than about ten.

The good agreement between the experimental ionisation energies and the values predicted by IMPACT indicates that the single-channel approximation is a reasonable one. This is because the configurations which can contribute to the ^{2}S ground state are widely separated in energy and the dominant configuration is the $1s^2 2s\ ^2S$, contributions from the nearest configurations being adequately accounted for through the bound channels. The same considerations apply to the continuum states and it can be expected that no significant errors are introduced into the calculations for the lithium-like ions through the use of only single-channel wavefunctions. This is confirmed by the results for O^{5+} at 1.5 and 2.5 times the ionisation energy which were obtained using the more complete five-state close-coupling wavefunctions (see table 9). The five-state results, however, do predict small changes in position and width of the resonances.

The comparison between the theoretical and experimental results is simpler in this case than for the beryllium-like ions since there is no contribution from metastables. The experiments show a marked increase in the cross section above about four times the ionisation energy due to the contribution of autoionisation, the relative importance of the effect increasing with the charge of the ion. Crandall *et al* (1979) have attributed the autoionisation to the states $1s2s^2\ ^2S$, $1s2s(^1S)2p\ ^2P$, $1s2s(^3S)2p\ ^2P$ and $1s2s2p\ ^4P$. In fact, at higher energies states of configurations $1s2lnl'$ ($l = 0, 1$, $l' < n$) will also contribute and could be accounted for in an appropriate multichannel calculation with

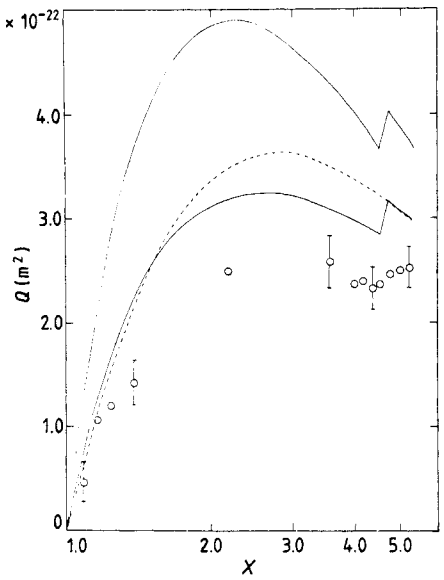

Figure 4. Ionisation cross section of C^{3+}. – – –, CBNX; —— (upper), CB; —— (lower), CBX. The experimental points are the crossed-beam data of Crandall *et al* (1979).

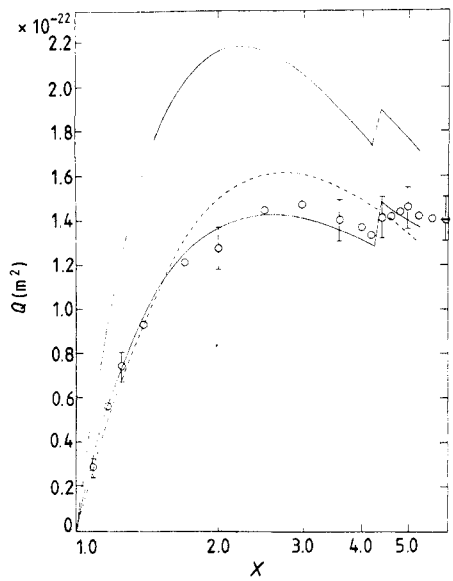

Figure 5. Ionisation cross section of N^{4+}. – – –, CBNX; —— (upper), CB; —— (lower), CBX. The experimental points are the crossed-beam data of Crandall *et al* (1979).

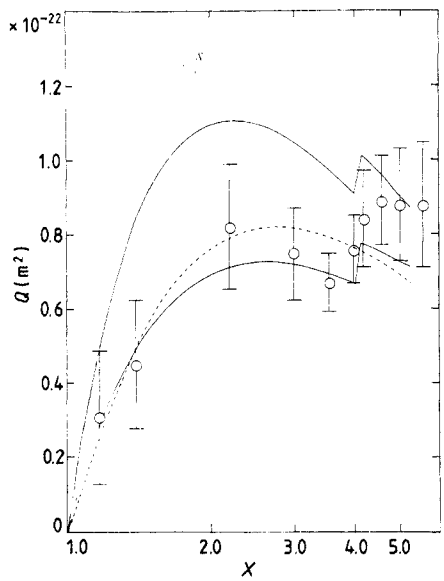

Figure 6. Ionisation cross section of O^{5+}. – – –, CBNX; —— (upper), CB; —— (lower), CBX. The experimental points are the crossed-beam data of Crandall *et al* (1979).

COBION as a manifestation of the mixing between open and closed channels. The metastable 1s2s2p ^{4}P state is of particular interest because it is forbidden in all the approximations discussed above since the $(N+1)$-electron system must have the same total spin as the ground state after the collision. These states can, however, be excited if the ionisation process is considered as an excitation of the three-electron ion by the

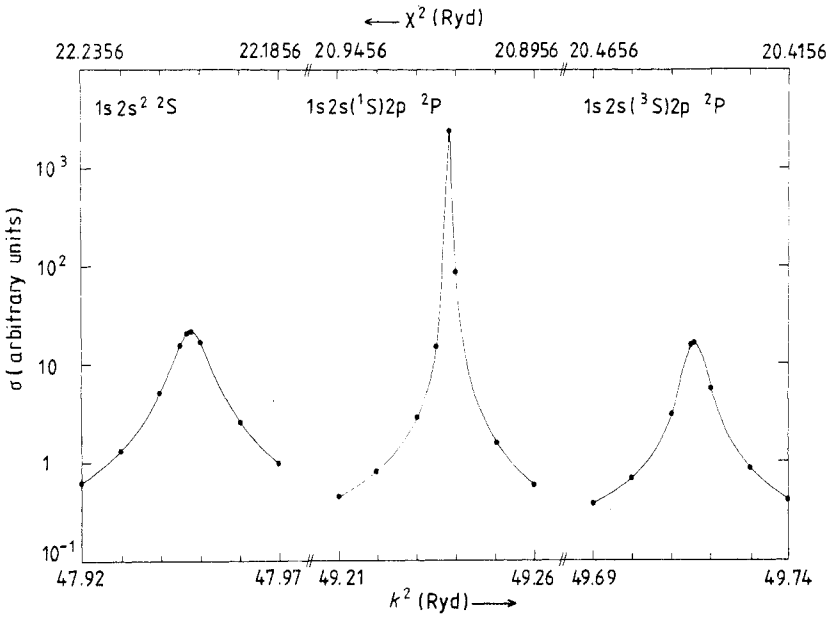

Figure 7. Calculated resonance structure in the differential cross section for ionisation of Ne^{7+} at an incident energy of five times the threshold energy. The points were calculated using the program COBION and the full curves were obtained using quantum defect theory and the program COBINT.

Table 11. Resonance positions for lithium-like ions in rydbergs.

Ion	C^{3+}		N^{4+}		O^{5+}		Ne^{7+}
Resonance	(a)	(b)	(a)	(b)	(a)	(b)	(a)
$1s2s^2\ ^2S$	21.409	21.510	30.211	30.341	40.450	40.603	65.521
$1s2s(^1S)2p\ ^2P$	22.102	22.184	31.158	31.088	41.429	41.495	66.813
$1s2s(^3S)2p\ ^2P$	22.418	22.547	31.442	31.501	41.849	41.955	67.290
$1s2p^2\ ^2S$	23.138	—	32.459	—	42.840	—	68.623

(a) This work.
(b) Henry (1979).

ionising electron, as in a conventional scattering calculation, with only one electron in the continuum in the final state, and would be included in a Coulomb–Born–Oppenheimer treatment of exchange. The corresponding excitation cross section is quite large (Henry 1979) and, because the lifetime of the state is very long and it is weakly coupled to the continuum, it is possible that this state contributes significantly to the autoionisation. The importance of this state should, however, decrease with increasing energy and Henry's results indicate that the dominant contribution is nevertheless from the $1s2s(^1S)2p\ ^2P$ state.

With the exception of C^{3+}, the agreement between the CBX results and experiment is good, although the large error limits in the O^{5+} results preclude any definite conclusions

from being made in this case. In the case of C^{3+} all the Coulomb–Born results, including those of Moores (1978), are consistently higher than experiment. It is reasonable to suppose, however, that the approximation will be least good for the lowest charged ion in the sequence. The CBX cross section in the autoionisation region for O^{5+} appears to be somewhat low compared with the measurements. One source of the discrepancy could be the omission of higher-lying autoionising states, although the results of Sampson and Golden (1979) would indicate that the effect of these states is small. Alternatively, the form of CBX used may be overestimating the effect of interference in this case. The results for Ne^{7+} indicate that the increase in importance of the autoionisation with increasing charge of the ion is not as great as predicted by Crandall *et al* (1979).

The results of Sampson and Golden (1979) are in very good agreement with those obtained here, despite the different physics of the two approaches. The Sampson and Golden approach uses scaled hydrogenic collision strengths, calculated for a theoretical ion with infinite nuclear charge, to obtain values of the appropriate excitation cross sections which are then added to the ionisation cross sections as calculated by a similar method using scaled hydrogenic cross sections (Golden and Sampson 1977). This method cannot account for the mixing between the excited state and continuum which is the source of the autoionisation. Another important difference between this method and the one presented here is that, whereas in calculating excitation cross sections to be added to an ionisation cross section a calculation of the scattering of an electron by an $(N+1)$-electron ion is carried out, when close-coupling wavefunctions are used to describe the $(N+1)$-electron system a calculation of the scattering by an N-electron ion is carried out. This means that in the limiting case of ionisation of neutral lithium, the excitation calculations would predict a zero contribution from the autoionisation at threshold while the method presented here would predict a finite contribution at threshold. An experimental test of this difference would be interesting.

Rate coefficients for lithium-like ions are given in table 12, which also shows the experimental data of Crandall *et al* (1979). For C^{3+} the present results and those from Sampson and Golden (1979) which are similar, give the best overall agreement with experiment. For N^{4+} our calculations are in excellent agreement with experiment below 10^6 K but at higher temperatures the Lotz formula takes over.

For O^{5+} the Coulomb–Born results are in better agreement than Lotz with experiment except between 1 and 6×10^6 K. For Ne^{7+} for which no crossed-beam results are available, the different theories give similar results. Also shown are results for Fe^{23+} computed from (5.3) which should give similar results to our method, and from (5.2). The Lotz result is again higher at high temperatures, again suggesting that the high-energy form of the Lotz cross section is inaccurate. In all cases the Lotz results, which do not include autoionisation, are larger than the others, which do include it.

In order to compare the results with plasma measurements of the rate coefficients, allowance should be made for the fact that if the plasma density is high the population of excited states may be significant (Crandall *et al* 1979) so that the quantity measured is not the pure ground-state ionisation rate coefficient. When this is done it is found that the results of Rowan and Roberts (1979) and Källne and Jones (1977) for N^{4+} and O^{5+}, allowing for experimental uncertainties, are in excellent agreement with our calculations. The results of Kunze (1971) for C^{3+}, N^{4+} and O^{5+}, however, appear to be rather low. The measurement of Jones *et al* (1977) for Ne^{7+} is also low whereas that of Hinnov (1966) is consistent with the calculations.

Table 12. Ionisation rate coefficients in 10^{-15} m^3 s^{-1}.

	C^{3+}				N^{4+}			
T (K)	JM	SG	L	E	JM	SG	L	E
2×10^5	0.046	0.052	0.058	0.042	0.003	0.004	0.004	0.003
4	0.372	0.399	0.464	0.292	0.070	0.076	0.084	0.070
6	0.763	0.799	0.952	0.612	0.203	0.215	0.242	0.202
1×10^6	1.38	1.41	1.71	1.14	0.484	0.505	0.580	0.487
2	2.16	2.19	2.70	1.87	0.969	0.988	1.14	1.00
4	2.72	2.67	3.38	2.44	1.38	1.39	1.62	1.52
6	2.83	2.78	3.60	2.77	1.53	1.55	1.82	1.76
1×10^7	2.81	2.75	3.69	3.04	1.61	1.62	1.96	2.01
2	2.56	2.49	3.55	2.89	1.55	1.56	1.98	2.01
5	2.06	2.00	3.08	2.64	1.30	1.31	1.80	1.79
1×10^8	1.66	1.62	2.64	2.32	1.07	1.08	1.54	1.53

	O^{5+}				Ne^{7+}		
T (K)	JM	SG	L	E	JM	SG	L
2×10^5	0.	0.	0.	0.	0.	0.	0.
4	0.012	0.013	0.014	0.013	0.	0.	0.
6	0.052	0.056	0.060	0.056	0.003	0.003	0.003
1×10^6	0.172	0.181	0.201	0.187	0.021	0.023	0.024
2	0.445	0.458	0.515	0.491	0.100	0.105	0.113
4	0.738	0.753	0.843	0.827	0.232	0.239	0.258
6	0.870	0.886	0.996	0.967	0.312	0.321	0.344
1×10^7	0.969	0.985	1.13	1.05	0.395	0.407	0.435
2	0.986	1.00	1.20	1.03	0.453	0.468	0.513
5	0.868	0.882	1.14	0.86	0.440	0.454	0.532
1×10^8	0.733	0.744	1.02	0.73	0.389	0.401	0.498

	Fe^{23+}	
T(K)	MGS	L
6×10^6	0.003	0.003
1×10^7	0.015	0.015
2	0.057	0.058
5	0.123	0.138
1×10^8	0.160	0.188
2	0.173	0.217
4	0.168	0.222
6	0.159	0.216
8	0.150	0.210
1×10^9	0.143	0.203

JM: this work.
MGS: Moores *et al* (1980).
L: Lotz (1968).
E: Crandall *et al* (1979).
SG: Sampson and Golden (1979).

7. Conclusions

The principal conclusions which may be drawn from this work are the following: the CB approximation is poor and overestimates the cross sections; CBNX gives reasonable results provided the energy is not such that autoionisation is important since it gives incorrect threshold energies. The CBX is the best of the Coulomb–Born approximations considered here. The infinite-Z method of Golden and Sampson gives a good approximation to the full CBX method if autoionisation (when necessary) is included in the former, even for C^{2+}. The effect of using distorted waves in place of Coulomb waves is to decrease the CBX results at low energies but away from threshold it is not of major importance in Li- and Be-like ions for which high partial waves, which are affected little by distortion, provide the principal contribution to the cross section. When one takes into consideration the fact that the experimental results contain an unknown contribution from metastable states, and may therefore be somewhat high, the agreement with experiment for Be-like ions is reasonably good.

For Li-like ions very good agreement is obtained with experiment for N^{4+} and O^{5+}; the C^{3+} CBX results are larger than experiment (see figure 4) by an amount increasing from threshold to about 20% at the peak. The autoionisation effects calculated here are at the same energy and of the same magnitude as predicted by experiment for C^{3+} and N^{4+} but the observed effect in O^{5+} is apparently underestimated by our calculations. A feature of the Coulomb–Born approximation is that the reduced cross section, obtained by multiplying the cross section by I^2 and dividing by the number of electrons in the shell being ionised, varies slowly along an isoelectronic sequence. Unlike theory the crossed-beam experimental results do not follow this scaling law very well. It is not clear whether this is due to the failure of the theoretical approximations for the low-charged ions or to experimental inaccuracies.

In all cases for $X < 5$, the agreement between the best DCBX calculation and the Lotz formula is better than about 25%. In view of the agreement with the crossed-beam experimental work, one is tempted to conclude that the results presented in this paper are correct to at least 20%, making a conservative estimate. On the other hand the ECIP method of Summers (1979) yields ground-state ionisation rates which are up to a factor of two smaller than those calculated by Jacobs *et al* (1977) using the Lotz formula. It is difficult to see how improvements to the present theory could bring the rates down by this amount.

In future calculations it is intended to extend the work to the case of ions with outer p electrons and to allow for the effect of closed channel resonances in the final state as well as bound channels.

Acknowledgements

The authors are indebted to Dr H Saraph whose program PHOTUC served as a model for COBION. Thanks are also due to Dr W Eissner not only for modifying the collision algebra code to do the Coulomb–Born algebra for us, but also for helpful advice in the running of the programs. HJ was supported by grants from the Science Research Council and from the Department of Physics and Astronomy, University College London.

References

Burgess A and Rudge M R H 1963 *Proc. R. Soc.* A **273** 372–86
Burgess A, Summers H P, Cochrane D M and McWhirter R W P 1977 *Mon. Not. R. Astron. Soc.* **179** 275–92
Burke P G and Seaton M J 1971 *Meth. Comput. Phys.* **10** 1–56
Cheng C C, Feldman U and Doschek G A 1979 *Astrophys. J.* **233** 736–40
Cowan R D and Mann J B 1979 *Astrophys. J.* **232** 940–7
Crandall D H, Phaneuf R A, and Gregory D C 1979 *Oak Ridge National Laboratory Report* No ORNL/TM-7020
Crees M A, Seaton M J and Wilson P M H 1978 *Comput. Phys. Commun.* **15** 23–83
Davies P C W and Seaton M J 1969 *J. Phys. B: At. Mol. Phys.* **2** 757–65
Dolder K T, Harrison M F A and Thonemann P C 1961 *Proc. R. Soc.* A **264** 367–78
Dubau J and Wells J 1973 *J. Phys. B: At. Mol. Phys.* **6** 1452–60
Edmonds A R 1960 *Angular Momentum in Quantum Mechanics* 2nd edn (Princeton, NJ: Princeton University Press)
Eissner W and Moores D L 1980 *private communication*
Eissner W and Nussbaumer H 1969 *J. Phys. B: At. Mol. Phys.* **2** 1028–43
Gabriel A H 1972 *Mon. Not. R. Astron. Soc.* **160** 99–119
Golden L A and Sampson D H 1977 *J. Phys. B: At. Mol. Phys.* **10** 2229–37
Hamdan M, Birkinshaw K and Hasted J B 1978 *J. Phys. B: At. Mol. Phys.* **11** 331–8
Henry R J W 1979 *J. Phys. B: At. Mol. Phys.* **12** L309–13
Hinnov E 1966 *J. Opt. Soc. Am.* **56** 1179
Jacobs V L, Davis J, Kepple P C and Blaha M 1977 *Astrophys. J.* **211** 605–16
Jakubowicz H 1980 *PhD Thesis* University of London
Jakubowicz H and Moores D L 1980 *Comm. At. Mol. Phys.* **9** No 2 55–70
Jones L A, Källne E and Thomson D B 1977 *J. Phys. B: At. Mol. Phys.* **10** 187
Jones M 1974 *Comput. Phys. Commun.* **7** 353–67
Jordan C 1970 *Mon. Not. R. Astron. Soc.* **148** 17–23
Källne E and Jones L A 1977 *J. Phys. B: At. Mol. Phys.* **10** 3637–48
Kim Y and Cheng K 1979 *Proc. 11th Int. Conf. on Physics of Electronic and Atomic Collisions, Kyoto* (Kyoto: Society for Atomic Collision Resarch)
Kim Y and Inokuti M 1971 *Phys. Rev.* A **3** 665–78
Kunze H J 1971 *Phys. Rev.* A **3** 937–42
Lotz W 1967 *Astrophys. J. Suppl.* **14** 207–38
—— 1968 *Z. Phys.* **216** 241–7
Moores D L 1978 *J. Phys. B: At. Mol. Phys.* **11** L403–5
—— 1979 *J. Phys. B: At. Mol. Phys.* **12** 4171–8
Moores D L, Golden L A and Sampson D H 1980 *J. Phys. B: At. Mol. Phys.* **13** 385–95
Moores D L and Nussbaumer H 1970 *J. Phys. B: At. Mol. Phys.* **3** 161–72
Peart B, Walton D S and Dolder K T 1969 *J. Phys. B: At. Mol. Phys.* **2** 1347–52
Peterkop R K 1961 *Proc. Phys. Soc.* **77** 1220
—— 1977 *Theory of Ionization of Atoms by Electron Impact* (Colorado: Associated University Press)
Pradhan A K 1980 *Mon. Not. R. Astron. Soc.* 58–88
Pradhan A K and Seaton M J 1981 to be published
Rowan W L and Roberts J R 1979 *Phys. Rev.* A **19** 90–8
Rudge M R H 1968 *Rev. Mod. Phys.* **40** 564–90
Rudge M R H and Schwartz S B 1966 *Proc. Phys. Soc.* **88** 563–78, 579–85
Rudge M R H and Seaton M J 1965 *Proc. R. Soc.* A **283** 262–90
Sampson D H and Golden L A 1979 *J. Phys. B: At. Mol. Phys.* **12** L785–91
Saraph H E 1981 *Comput. Phys. Commun.* submitted for publication
Seaton M J 1964 *Planet. Space Sci.* **12** 55–74
—— 1974 *J. Phys. B: At. Mol. Phys.* **7** 1871–40
—— 1978 *J. Phys. B: At. Mol. Phys.* **11** 4067–93
Summers H P 1974 *Mon. Not. R. Astron. Soc.* **169** 663–80
—— 1979 *Appleton Laboratory Report* AL-R15
Woodruff P R, Hublet M C and Harrison M F A 1978 *J. Phys. B: At. Mol. Phys.* **11** L305–8
Younger S M 1980a *Phys. Rev.* A **22** 111–7
—— 1980b *Phys. Rev.* A **22** 1425–31